Significance of an amorphous SiO_2 phase in a pseudomorph after coesite enclosed in garnet from ultrahigh-pressure eclogite, Su-Lu Belt, eastern China

Tomoki Taguchi[1*], Akira Miyake[2], Masaki Enami[1], Yohei Igami[2]

[1] Institute for Space–Earth Environmental Research, Nagoya University, Furo-cho, Chikusa-ku, Nagoya 464-8601, Japan

[2] Department of Geology and Mineralogy, Graduate School of Science, Kyoto University, Kitashirakawa Oiwake-cho, Sakyo-ku, Kyoto 606-8502, Japan

* Present address: Department of Geology and Mineralogy, Graduate School of Science, Kyoto University, Kitashirakawa Oiwake-cho, Sakyo-ku, Kyoto 606-8502, Japan

Corresponding author: Tomoki Taguchi

E-mail address: taguchi-tomoki@kueps.kyoto-u.ac.jp

ABSTRACT

Here we report the first discovery of an amorphous SiO_2 phase (APSI phase) in a pseudomorph after coesite included in garnet from an ultrahigh-pressure (UHP) eclogite from the Su-Lu metamorphic belt, eastern China. Using transmission electron microscopy, Raman spectroscopy and selected area electron diffraction, we show that the internal structure of the pseudomorph consists of an APSI phase with nano/submicrocrystalline particles of quartz and a polycrystalline K-bearing fibrous sheet-silicate phase (KFSS phase). The APSI phase-bearing aggregates included in the garnet might have formed by reactions involving a supercritical fluid during exhumation by the following processes: (1) the development of radial cracks within the host garnet by the phase transition of coesite to quartz; (2) the decomposition of a part of the pseudomorph following infiltration of supercritical fluid; (3) the precipitation of the KFSS phase from the fluid phase during subsequent exhumation and cooling, which was likely promoted by a change in the metamorphic fluid from supercritical and/or subcritical to aqueous fluid; and, (4) the rapid precipitation of the APSI phase under a metastable (non-equilibrium) state, such as quenching, during a later stage of the exhumation. Whether the APSI phase generally formed

during exhumation and survived widely throughout the Su-Lu terrane is unknown. However, the presence of the APSI phase in a UHP eclogite provides new insight into the geodynamic phenomena occurring at continental collision zones.

KEYWORDS: amorphous SiO_2 phase, metamorphic fluid, pseudomorph after coesite, Su-Lu Belt, TEM observation

1 | INTRODUCTION

Coesite, the high-pressure polymorph of SiO_2, has been identified in continental collision related metamorphic rocks (Chopin, 1984; Smith, 1984). The appearance of coesite is considered to be an indicator of ultrahigh-pressure (UHP) metamorphism, and is evidence that crustal materials have experienced conditions of P >2.8 GPa (e.g. Liou, Zhang, Ernst, Rumble, & Maruyama, 1998). The estimated peak pressure condition is generally interpreted to reflect the maximum depth of burial of the rocks, and the coesite-bearing UHP rocks are considered to have reached mantle depths (>80 km) before return to the Earth's surface. However, some recent studies present an alternative view suggesting that coesite could have formed at shallower depths under deviatoric stress conditions, as proposed by recent models for the development of overpressures at the micro to macro scales (e.g., Schmalholz & Podladchikov 2014; Schmalholz, Medvedev, Lechmann, & Podladchikov, 2014; Angel, Nimis, Mazzucchelli, Alvaro, & Nestola, 2015; Gerya, 2015). In any case, the discovery of UHP minerals in metamorphic rocks would be key for metamorphic petrology and geodynamic reconstructions (Chopin, 1984, 2003).

Most coesite grains, however, have been transformed into quartz-pseudomorphs, which preserve geological and mineralogical information useful for understanding the exhumation process. Generally, pseudomorphs after coesite are composed of polycrystalline quartz grains and have developed radial fractures in the enclosing garnet or other mechanically strong phases (e.g., Chopin, 1984, 2003; Gillet, Ingrin, & Chopin, 1984), although occurrences with K-feldspar in pseudomorphs have also been reported (e.g., Enami & Zang 1990; Enami, Zang, & Yin, 1993; Yang, Godard, & Smith, 1998). Yang et al. (1998) reported polycrystalline sanidine or orthoclase in quartz pseudomorphs after coesite in omphacite grains of Su-Lu UHP rocks and proposed a hypothesis that the K-feldspar formed by reaction between the $KAlSi_2O_6$ component exsolved from K-bearing omphacite and the SiO_2 phase in the pseudomorph. Recently, however,

pseudomorphs consisting of quartz + K-feldspar ± albite assemblages have been interpreted to have crystallized from high-pressure melts (Gao, Zheng, & Chen, 2012; Gao, Zheng, Chen, & Hu, 2013; Liu, Hermann, & Zhang, 2013; Sheng, Zheng, Li, & Hu, 2013; Wang et al., 2014). In addition, Yang, Huang, Wu, & Zhang (2014a) and Yang, Fan, Yu, & Yan (2014b) suggested that K-feldspar-bearing quartz pseudomorphs might be rapidly crystallized products of coseismic pseudotachylyte. The textural characteristics and mineral paragenesis of polyphase pseudomorphs might be among the new critical indicators in understanding the kinetics of UHP metamorphism, fluid–melt activity, and the exhumation process of UHP rocks. However, solidified melt inclusions are generally composed of various minerals including mafic phases occurring as negatively shaped crystals, and have been detected in felsic lithologies (Cesare, Ferrero, Salvioli-Mariani, Pedron, & Cavallo, 2009). Explaining the origin of simple aggregates of felsic phases in mafic eclogites may be more difficult, because the mineralogical data may be insufficient, and the origin of such aggregates has not yet been well understood.

Using a transmission electron microscope (TEM) and Raman spectroscopy, we carefully studied pseudomorphs after coesite in garnet from a UHP eclogite from Yangzhuang in the Junan region of eastern China, part of the Su-Lu Belt, and confirmed that the pseudomorph consists of amorphous SiO_2 (APSI) and K-bearing fibrous sheet-silicate (KFSS) phases. To the best of the authors' knowledge, the existence of fine aggregates with an amorphous SiO_2 phase and a sheet-silicate phase has never been reported from any UHP metamorphic rocks. In this study, we report on the crystal chemical features and nano-textural characteristics of the pseudomorph, consisting of the APSI phase and the KFSS phase, and discuss its origin and the implications for the behavior of metamorphic fluids.

2 | GEOLOGICAL OUTLINE AND SAMPLE DESCRIPTION

The Su-Lu terrane on the Shandong Peninsula of eastern China is bounded by the Wulian–Qingdao–Yantai Fault on its northwestern side and the Jiashan–Xiangshui Fault on its southeastern side. It is divided into two fault-bounded belts—a UHP belt and a high-pressure (HP) belt (Figure 1). The Su-Lu terrane is thought to have originated as part of the Yangtze Craton and to have undergone UHP–HP metamorphism when it was subducted below the Sino–Korean Craton during the Triassic period (240–220 Ma; e.g., Hacker, Wallis, McWilliams, &

Gans, 2009). Coesite and quartz-pseudomorphs after coesite are widespread in eclogites and their country orthogneisses (e.g., Yang & Smith, 1989; Enami & Zang, 1990; Hirajima et al., 1990; Okay, Xu & Sengör, 1989; Wang, Liou & Mao, 1989; Ye et al., 2000).

The Yangzhuang UHP eclogite body of the Junan region is situated at the southwestern part of the UHP sector of the Su-Lu Belt (longitude 118° 51' 06" E and latitude 35° 02' 34" N). The exposed eclogite body is approximately 10 m in width and is composed of alternations of zoisite-rich and omphacite-rich eclogite layers. Direct contact between the country orthogneiss and the eclogite is not observed. Other petrological and geological characteristics of the Yangzhuang eclogite are well documented by Enami and Nagasaki (1999) and Taguchi, Enami, and Kouketsu (2016). Garnet exhibits discontinuous zoning with inner and outer generations of growth. The inner segment shows normal zoning with a monotonous grossular decrease from the center toward the margin, and contains α-quartz as inclusions. The outer segment surrounds the inner segment discontinuously and rarely includes coesite and quartz pseudomorphs after coesite. Equilibrium conditions of the inner and outer segments were estimated as 1.3–2.3 GPa/500–630 °C and 3.1 GPa/660–725 °C, respectively (Taguchi et al. 2016).

The sample investigated in this study (95ZYa) was collected from a zoisite-rich eclogite layer. Nagasaki (1997) reported the bulk-rock composition of sample 95ZYa, which is given in Table 1. The Al-rich bulk-rock composition implies that the protolith of the UHP eclogite comprised a mixture of basalts and clay-rich sediments (Enami & Nagasaki, 1999). The eclogite sample 95ZYa is composed of garnet, omphacite, zoisite, phengite, amphibole, kyanite and quartz, with small amounts of apatite and rutile. The mode was determined by point counting (1000 points per sample, X= 0.5 mm, Y= 0.5 mm) using an optical microscope. The major phases are zoisite, garnet, quartz and phengite, which make up 32.3, 20.2, 18.5 and 16.2 vol%, respectively, with minor omphacite, kyanite, amphibole and accessory phases constituting 5.2, 3.8, 3.2 and 0.6 vol%, respectively. Garnet porphyroblasts are mostly 1 mm in diameter or larger. They show chemical zoning similar to those in other Yangzhuang eclogites (e.g., Taguchi et al., 2016). This zoning can be divided into inner and outer segments (Figure 2a). The boundary of the inner and outer segment is marked by a minimum grossular content of approximately 22 mol% (Figure 2b). In the inner segment, the pyrope content monotonously increases from the center toward the margin. In contrast, the almandine content exhibits a mosaic texture consisting of

several irregular almandine-rich domains (Figure 2a). The representative inclusion assemblage in the inner segment of the garnet is α-quartz + zoisite + rutile + paragonite. In the inner segment, the SiO_2 is all α-quartz with no coesite present or radial cracks observed. In contrast, kyanite with coesite inclusions was observed as an inclusion in the outer segment of the garnet (Figure 2c, d). The outer segment contains eclogite and UHP minerals as inclusions including pseudomorphs after coesite with omphacite + kyanite + phengite + rutile + zoisite.

3 | ANALYTICAL PROCEDURES

Textural characteristics of the pseudomorph studied in detail were observed using a field emission-scanning electron microscope (FE-SEM; SU6600, Hitachi High-Tech) operated at 15 kV at Nagoya University. The chemical compositions of minerals were derermined using an electron probe microanalyzer with wavelength- and energy-dispersive systems (JXA-8900R, JEOL) at Nagoya University. The operating conditions were a 15 kV accelerating voltage, a 12 nA beam current, and a 2–3 μm beam spot diameter. The abbreviations for minerals and end-member components follow Whitney and Evans (2010).

Minerals and amorphous phases were identified using a laser Raman spectrometer (Nicolet Almega XR, Thermo Fisher Scientific K.K.) at Nagoya University. The instrument was equipped with a 532-nm Nd–YAG laser, a charge-coupled device (CCD) detector with 256 × 1024 pixels cooled by a Peltier element, and an automated confocal microscope (BX51; Olympus). The objective was an Olympus MplanBD 100X lens with a numerical aperture of 0.9. The spatial resolution was approximately 0.6 μm, and the laser had a maximum power of 25 mW. The pinhole diameter was 25 μm, and the corresponding wavenumber resolution was approximately 1.1–1.3 cm^{-1} in the spectral range with a grating of 2400 lines per mm. The spectrometer was calibrated using Ne lines. The room temperature was maintained at 22 ± 1 °C.

An ultra-thin section of the pseudomorph was made using a focused ion beam (FIB) system (Quanta 200 3DS, FEI) at Kyoto University. A predefined area (~30 μm^2) was coated with platinum (Pt) and the surrounds cut out to a depth of ~10 μm using a gallium (Ga) ion beam. Afterwards, the resulting foil was picked up by an *in situ* Omniprobe inside the FIB and then mounted on a TEM grid. The extracted sample was thinned to 100–200 nm using a Ga ion beam at 30 kV with beam currents ranging from 0.1 nA to 30 nA and at 5 kV with a beam current of

16 pA for the final processing. The sample was studied using a transmission electron microscope (TEM) equipped with an energy-dispersive spectroscopy (EDS) system operating at 200 kV at Kyoto University (JEM-2100F, JEOL). TEM images were recorded using a CCD camera (Orius200D, Gatan).

4 | POLYPHASE PSEUDOMORPH

Pseudomorphs after coesite are generally composed of polycrystalline quartz and have been commonly described as quartz pseudomorphs (e.g., Chopin, 1984; 2003). However, the pseudomorph we have studied in detail, which we will refer to as "the pseudomorph" hereafter, consists of aggregates of SiO_2 phases and K-bearing silicates. Figures 2e and 3 show the textural and elemental features of the pseudomorph, which is approximately120 μm across and is located in the outer segment of the host garnet. Radial cracks develop in garnet around the pseudomorph (Figure 3a–c). The pseudomorph is divided into dark-colored and transparent areas under plane-polarized light, which dominate primarily the core and margin, respectively (Figure 3a). The transparent areas under plane-polarized light correspond with areas of polycrystalline SiO_2 phases under cross-polarized light (Figure 3b). In contrast, the dark-colored area under plane-polarized light consists of very fine-grained aggregates of an SiO_2 phase and a fibrous phase containing K and Mg (Figure 3c–f).

Figure 4 shows Raman spectra of the SiO_2 phases (Spots 1 and 2) in the dark-colored area of the pseudomorph. The Raman spectrum of a single α-quartz crystal measured under the same equipment and conditions and the Raman spectrum of SiO_2 glass, reported by Ivanda, Clasen, Hornfeck, and Kiefer (2003), are also shown in Figure 4 for comparison. The SiO_2 phases at both spots 1 and 2 show broad Raman spectra with weak bands near 459 and 602 cm^{-1}, but they do not show any definitive Raman bands of α-quartz at 128, 205 and 464 cm^{-1}. The fibrous phase has a broad Raman spectrum and never shows a distinctive Raman band (Spot 3 in Figure 4). Kyanite with a coesite inclusion was identified in the outer segment of the garnet (Spot 4 in Figure 4).

A selected portion of the dark-colored area under plane-polarized light cut out by the FIB (Figure 3f). Figure 5a, b shows the bright field (BF)-TEM image and the high-angle annular dark field scanning TEM (HAADF-STEM) image of a cross-section (~15 μm × ~10 μm) of the coupled chip, respectively, implying that the dark-colored area is composed of worm-like

massive and fibrous parts. The HAADF-STEM image (Figure 5b) shows that the massive part is compositionally homogeneous. The TEM-EDS spectrum (Figure 5c) shows that the massive part (Figure 5e) has a nearly pure SiO_2 composition, and the fibrous part (Figure 5h) is a KFSS phase. The bright field mode of the micro/nanostructure of the SiO_2 and KFSS phases and the selected area electron diffraction (SAED) patterns are shown in Figure 5d–h. The SAED analyses of most of the worm-like SiO_2 phase did not show any diffraction spots (Figure 5d, e), suggesting a non-crystalline state. These APSI phases sometimes include nanoparticles with an SiO_2 composition. The SAED pattern of the nanoparticles (Figure 5f) could be indexed as quartz along the $[10\bar{3}]$ zone axis, displaying 010 and $3\bar{1}1$ spots. The submicron particles of the SiO_2 phase also occur in the aggregates of the KFSS phases (Figure 5g), having the SAED pattern indexed as quartz along the $[12\bar{2}]$ zone axis, displaying $2\bar{1}0$ and 011 spots. The SAED analysis of fibrous minerals shows a weak ring pattern (Figure 5h), and the corresponding d-values are approximately 4.8, 4.3, and 2.5 Å. From these d-values and the EDS analysis data, the fibrous minerals could be identified as polycrystalline KFSS phases.

5 | DISCUSSION

The transformations of α-quartz and coesite into an APSI phase were experimentally replicated at 25–35 GPa and 300 K (Hemley, Jephcoat, Mao, & Ming, 1988). Hazen, Finger, Hemley, and Mao (1989) considered that the amorphization starts at 12.5 GPa and is nearly complete at 15.3 GPa at 300 K. This phenomenon is known as pressure-induced amorphization and requires a process with an instantaneous pressure increase. Recently, examples of the disordered and incipient APSI phase, which are simply denoted as "the incipient APSI phase" hereafter, have been found as inclusions completely enclosed in omphacite and/or garnet in HP–UHP metamorphic rocks from Antarctica (Palmeri, Frezzotti, Godard, & Davies, 2009) and the western Alps (Frezzotti, Palmeri, Ferrando, Compagnoni, & Godard, 2015). Using Raman spectroscopy and X-ray micro-diffraction, Palmeri et al. (2009) suggested that shock metamorphism or local overpressure (> 15 GPa) at an inclusion scale might have caused amorphization of a monocrystalline SiO_2 phase in eclogites during the prograde metamorphic stage. The incipient APSI phase shows Raman bands of 480–485, 520–523, and 807 cm^{-1} in addition to those of α-quartz (Palmeri et al. 2009). The Raman band of 520–523 cm^{-1} corresponds

to the four-membered rings of a corner-sharing SiO_4 tetrahedron of the coesite (Kingma & Hemley 1994). The incipient APSI phase characteristically shows high intensity ratios I_{265}/I_{465} and I_{402}/I_{465}, where I_ν indicates the intensity of the Raman band ν (Palmeri et al. 2009; Godard, Frezzotti, Palmeri, & Smith, 2011). In contrast to the incipient APSI phase, the APSI phase of the Yangzhuang sample described in this study does not show any Raman bands assigned to those of α-quartz and coesite (Spots 1–2 in Figure 4). The weak band at 602 cm^{-1} can be assigned to the symmetric stretching vibration of Si-O in a planar three-membered SiO_4 ring (D_2 band) of amorphous SiO_2 glass (Awazu & Kawazoe 2003; Ivanda et al., 2003). Raman spectra, TEM observation, and SAED analysis (Figure 5d, e) suggest that the APSI phase in the studied sample is almost entirely in an amorphous state, unlike the incipient APSI phase reported from the Antarctica (Palmeri et al., 2009) and the western Alps (Frezzotti et al., 2015) samples.

Pseudomorphs composed of the quartz + K-feldspar ± albite are commonly identified as transformation products from coesite. In this regard, the origin has been recently discussed to explain the formation of such inclusions as follows: (1) K-feldspar formed by reaction between a $KAlSi_2O_6$ component exsolved from K-bearing omphacite and an SiO_2-phase in the pseudomorph after coesite (Yang et al., 1998); (2) breakdown and reaction products of former UHP phases such as coesite + K-cymrite (Massone, 2001; Massone & Nasdala, 2003; Zhang et al., 2009); (3) the quartz + K-feldspar ± albite assemblage is not a pseudomorph after coesite, but rather a melting product of phengite in UHP eclogites (Gao et al., 2012, 2013; Liu et al. 2013; Sheng et al. 2013; Chen, Zheng, Gao, & Hu, 2014; Wang et al., 2014); (4) K-feldspar-bearing inclusions might be rapidly crystallized products derived from phengite due to frictional heating (Yang et al., 2014a, b); and (5) multi-solid phase inclusions in garnet crystallized from Si-, Mg-, and K-rich fluid under peak UHP metamorphic conditions (e.g., Ferrando, Palmeri, Dallai, & Compagnoni, 2005; Wang, Wang, Brown, & Feng, 2016). Ferrando et al. (2005) reported occurrences of multi-phase solid inclusions in quartzite and eclogite from the Donghai area of the Su-Lu UHP metamorphic terrane, which is situated approximately 60 km south of the Yangzhuang area. In the case of the Donghai samples, the various polyphase mineral association of rhombic- and/or negatively shaped crystals are 1) paragonite + muscovite + anhydrite ± corundum ± sulfate ± zircon ± calcite ± chlorite ± SiO_2 phase ± barite ± pyrite ± apatite in quartzite, and 2) paragonite + rutile + apatite ± amphibole ± Zn-staurolite ± magnetite ± plagioclase

± zircon ± pyrite ± sulphate ± spinel in eclogite. They suggested that the multiphase solid inclusions were remnants of extensive activity of supercritical silicate-rich aqueous fluids during the peak metamorphic stage. Recently, however, a prevailing theory of the origin of the quartz + K-feldspar ± albite assemblage suggests that they likely crystallized from felsic melts due to dehydration melting of phengite (e.g., Gao et al., 2012; Liu et al, 2013) or frictional heating of phengite caused by seismic waves (Yang et al., 2014b; Yang, Zhang, Chen, & Huang, 2017). The major-element composition of the host garnet or omphacite is homogeneous, suggesting that the melts were not produced by infiltration of external felsic melts (Gao et al., 2012; Gao, Chen, & Zhang, 2017). However, previous studies have not confirmed the aggregate, including the entire amorphous SiO_2 phase.

In this study, kyanite with relict coesite occurred only as an inclusion in the outer segment of the garnet (Figure 4). The pseudomorph with numerous radial cracks also occurs only in the outer segment of the garnet (Figure 2a, e), and it is divided into the core, consisting of APSI and KFSS phases, and the surrounding mantle of polycrystalline quartz. The occurrence of relict coesite and pseudomorphs after coesite in the outer segment of the garnet provides clear evidence that the pressure conditions of the Yangzhuang sample reached the coesite stability field. The APSI phase coexisting with the KFSS phase in the pseudomorph seems to have formed in an open system after the transformation of coesite to quartz during the exhumation stage and might also provide clues to the interpretation of the formation process of the pseudomorph.

In the Yangzhuang sample, the APSI and KFSS phases do not occur as negatively shaped crystals, and the common aggregate included in the pseudomorph is SiO_2 (APSI phase + quartz) + KFSS phases and is a very simple association. In addition, phengite-breakdown textures such as K-feldspar + quartz are not observed in the garnet (Figure 2e). Thus, the Yangzhuang pseudomorph is difficult to interpret simply as a remnant of partial melt. In this study, relict coesite grains are not confirmed in the pseudomorph, which implies that the coesite to quartz transformation was complete. The presence of an aqueous fluid phase at the inclusion–host mineral boundaries promotes the transformation of coesite (Mosenfelder & Bohlen, 1997; Liou et al. 1998; Lathe et al. 2005; Mosenfelder, Schertl, Smyth, & Liou, 2005). Infiltration of a fluid phase might have played an important role in the formation of the polyphase pseudomorph after coesite in the case of the Yangzhuang sample. Consequently, the APSI phase and the coexisting

phases in the Yangzhuang sample are considered to have formed by the following process, as shown in Figure 6a, b. First, radial cracks developed in the garnet during the exhumation and formation of the pseudomorph, consisting of a coesite core and a quartz mantle (stage 1). Such a two-component texture of pseudomorphs after coesite is generally recognized in UHP metamorphic rocks (e.g., Liou et al. 1998). Second, the metastable coesite core selectively decomposed through the infiltration of a K-rich supercritical metamorphic fluid (stage 2). A K-rich, SiO_2-rich fluid is common in UHP metamorphic terranes as shown by several studies based on the fluid and solid nanoinclusions in microdiamond (e.g., Dobrzhinetskaya, 2012; Dobrzhinetskaya, Wirth, Green, Schreiber, & O'bannon, 2013; Jacob, Dobrzhinetskaya, & Wirth, 2014). During the subsequent exhumation and cooling stage, the KFSS phases precipitated from the K-rich, SiO_2-rich metamorphic fluid (stage 3), which could have been promoted by the state change of the metamorphic fluid from supercritical to subcritical and/or aqueous fluid. Finally, rapid precipitation of the APSI phase under the metastable (non-equilibrium) state, such as quenching, started during a late stage of exhumation (stage 4). Although the origin of nano/submicrocrystalline quartz grains in the APSI phase (Figure 5f, g) is not conclusive, the grains are probably undissolved residual quartz crystals, which are part of the former pseudomorph after coesite.

Our interpretation might suggest that the APSI phase did not form due to the pressure-induced amorphization process proposed by the studies on the Antarctica (Palmeri et al. 2009) and western Alps (Frezzotti et al. 2015) samples. The Yangzhuang sample suggests that metamorphic fluid might have strongly controlled the transition of coesite and the formation of various types of polyphase pseudomorphs during a later stage of exhumation. The APSI and the KFSS phases did not recrystallize to quartz and mica during the long processes of the exhumation stage. This indicates that duration of the exhumation did not provide enough time to convert the APSI phase to a crystalline SiO_2 phase. The geochemical understanding of kinetics for silica polymorph precipitation is based on a few well-controlled laboratory experiments (e.g., Rimstidt & Barnes, 1980; Renders, Gammons, & Barnes, 1995). However, the precipitation processes of an entire amorphous and almost pure SiO_2 phase that are acquired upon cooling are poorly understood. Laboratory experiments form the basis for models of silica reaction kinetics; however, they may insufficiently describe more complex natural systems. The most common

means of experimentally forming amorphous material is by quenching a liquid rapidly to avoid crystallization (e.g., Debenedetti & Stillinger, 2001). The occurrence of a relict APSI phase indicates that the Yangzhuang eclogites have not experienced environments that promote recrystallization from the APSI phase to crystalline quartz, and therefore a quenching process appears to be necessary.

Probable quench textures (intergranular coesite, microlites, etc.) have been recently reported in a coesite-bearing eclogite breccia in the Yangkou area of the Su-Lu terrane (Yang et al., 2014b). It is not clear at the current moment whether the occurrence of the APSI phase and/or the presence of the quenching process is a localized phenomenon or extends throughout the Su-Lu UHP terrane. However, the results of this study provide new insights into the geological processes occurring at continental collision zones and might play a critical role in understanding the kinetic significance of amorphous and poorly crystallized materials in natural environments. Petrologists should therefore focus on pseudomorphs after coesite in mechanically strong minerals from a nanoscale viewpoint, to understand the history of fluid activity and the cooling process during the exhumation of UHP rocks using FIB, TEM, and other analytical techniques.

ACKNOWLEDGEMENTS

We are grateful to T. Nishiyama and L. Dobrzhinetskaya for their careful reading and useful suggestions that led to a considerable improvement in the manuscript. We also thank M. Brown for the editorial handling of this paper and comments that helped improve the manuscript. We deeply thank J. -J. Yang for the careful reading and providing many valuable comments on earlier version of this manuscript. The first author thanks M. Satish-Kumar at Niigata University for useful comments that were helpful in improving the manuscript and also appreciates the help of S. Hayashi at Nagoya University for his technical assistance during the FE-SEM observations. We acknowledge A. Nagasaki (Okubo) for permitting us to cite her unpublished bulk-rock composition of the sample 95ZYa. Sincere thanks are also extended to S. Wallis and members of the petrology group at Nagoya University for numerous discussions. This study was financially supported by a Research Fellowship for Young Scientists (Taguchi: 15J04749, 17J04059) from the Japan Society for the Promotion of Science (JSPS).

REFERENCES

Angel, R. J., Nimis, P., Mazzucchelli, M. L., Alvaro, M., & Nestola, F. (2015). How large are departures from lithostatic pressure? Constraints from host–inclusion elasticity. *Journal of Metamorphic Geology*, *33*, 801–813.

Awazu, K., & Kawazoe, H. (2003). Strained Si–O–Si bonds in amorphous SiO_2 materials: a family member of active centers in radio, photo, and chemical responses. *Journal of Applied physics*, *94*, 6243–6262.

Cesare, B., Ferrero, S., Salvioli-Mariani, E., Pedron, D., & Cavallo, A. (2009). "Nanogranite" and glassy inclusions: The anatectic melt in migmatites and granulites. *Geology*, *37*, 627–630.

Chen, Y. X., Zheng, Y. F., Gao, X. Y., & Hu, Z. (2014). Multiphase solid inclusions in zoisite-bearing eclogite: evidence for partial melting of ultrahigh-pressure metamorphic rocks during continental collision. Lithos, 200, 1–21.

Chopin, C. (1984). Coesite and pure pyrope in high-grade blueschists of the Western Alps: a first record and some consequences. *Contributions to Mineralogy and Petrology*, *86*, 107–118.

Chopin, C. (2003). Ultrahigh-pressure metamorphism: tracing continental crust into the mantle. *Earth and Planetary Science Letters*, *212*, 1–14.

Debenedetti, P. G., & Stillinger, F. H. (2001). Supercooled liquids and the glass transition. *Nature*, *410*, 259–267.

Dobrzhinetskaya, L. F. (2012). Microdiamonds–Frontier of ultrahigh-pressure metamorphism: A review. *Gondwana Research*, *21*, 207–223.

Dobrzhinetskaya, L. F., Wirth, R., Green, H. W., Schreiber, A., & O'bannon, E. (2013). First find of polycrystalline diamond in ultrahigh-pressure metamorphic terrane of Erzgebirge, Germany. *Journal of Metamorphic Geology*, *31*, 5–18.

Enami, M., & Zang, Q. (1990). Quartz pseudomorphs after coesite in eclogites from Shandong province, east China. *American Mineralogist*, *75*, 381–386.

Enami, M., Zang, Q., Yin, Y. (1993). High-pressure eclogites in northern Jiangsu–southern Shandong province, eastern China. *Journal of Metamorphic Geology*, *11*, 589–603.

Enami, M., & Nagasaki, A. (1999). Prograde P–T path of kyanite eclogites from Junan in the Sulu ultrahigh-pressure province, eastern China. *Island Arc*, *8*, 459–474.

Ferrando, S., Frezzotti, M. L., Dallai, L., & Compagnoni, R. (2005). Multiphase solid inclusions in UHP rocks (Su-Lu, China): Remnants of supercritical silicate-rich aqueous fluids released during continental subduction. *Chemical Geology*, *223*, 68–81.

Frezzotti, M. L., Palmeri, R., Ferrando, S., Compagnoni, R., & Godard, G. (2015) α-quartz in UHP rocks: irrelevant or crucial? In: XI International Eclogite Conference, pp. 38, Dominican Geological Survey, Dominican Republic.

Gao, X. Y., Zheng, Y. F., & Chen, Y. X. (2012). Dehydration melting of ultrahigh-pressure eclogite in the Dabie orogen: evidence from multiphase solid inclusions in garnet. *Journal of Metamorphic Geology*, *30*, 193–212.

Gao, X. Y., Zheng, Y. F., Chen, Y. X., & Hu, Z. (2013). Trace element composition of continentally subducted slab-derived melt: insight from multiphase solid inclusions in ultrahigh-pressure eclogite in the Dabie orogen. *Journal of Metamorphic Geology*, *31*, 453–468.

Gao, X. Y., Chen, Y. X., & Zhang, Q. Q. (2017). Multiphase solid inclusions in ultrahigh-pressure metamorphic rocks: A snapshot of anatectic melts during continental collision. *Journal of Asian Earth Sciences*, 145, 192–204.

Gerya, T. (2015). Tectonic overpressure and underpressure in lithospheric tectonics and metamorphism. *Journal of Metamorphic Geology*, *33*, 785–800.

Gillet, P., Ingrin, J., & Chopin, C. (1984). Coesite in subducted continental crust: PT history deduced from an elastic model. *Earth and Planetary Science Letters*, *70*, 426–436.

Godard, G., Frezzotti, M. L., Palmeri, R., & Smith, D. C. (2011). Origin of high-pressure disordered metastable phases (lonsdaleite and incipiently amorphized quartz) in metamorphic rocks: Geodynamic shock or crystal-scale overpressure? In Dobrzhinetskaya, L. F., Faryad, S. W., Wallis, S., & Cuthbert, S., Eds., Ultrahigh-Pressure Metamorphism 25 Years after the Discovery of Coesite and Diamond, 125-148, Elsevier, Amsterdam.

Hacker, B. R., Wallis, S. R., Mcwilliams, M. O., & Gans, P. B. (2009). $^{40}Ar/^{39}Ar$ Constraints on the tectonic history and architecture of the ultrahigh-pressure Sulu orogen. *Journal of Metamorphic Geology*, *27*, 827–844.

Hazen, R. M., Finger, L. W., Hemley, R. J., & Mao, H. K. (1989). High-pressure crystal chemistry and amorphization of α-quartz. *Solid State Communications*, *72*, 507–511.

Hemley, R. J., Jephcoat, A. P., Mao, H. K., Ming, L. C., & Manghnani, M. H. (1988). Pressure-induced amorphization of crystalline silica. *Nature*, *334*, 52–54.

Hirajima, T., Ishiwatari, A., Cong, B., Zhang, R., Banno, S., & Nozaka, T. (1990). Coesite from Mengzhong eclogite at Donghai county, northeastern Jiangsu province, China. *Mineralogical Magazine*, *54*, 579–583.

Holland, T. J. B., & Powell, R. (1998). An internally consistent thermodynamic data set for phases of petrological interest. *Journal of metamorphic Geology*, *16*, 309–343.

Ivanda, M., Clasen, R., Hornfeck, M., & Kiefer, W. (2003). Raman spectroscopy on SiO_2 glasses sintered from nanosized particles. *Journal of non-crystalline solids*, *322*, 46–52.

Jacob, D. E., Dobrzhinetskaya, L., & Wirth, R. (2014). New insight into polycrystalline diamond genesis from modern nanoanalytical techniques. *Earth-Science Reviews*, *136*, 21–35.

Kingma, K. J., & Hemley, R. J. (1994). Raman spectroscopic study of microcrystalline silica. *American Mineralogist*, *79*, 269–273.

Lathe, C., Koch-Müller, M., Wirth, R., Westrenen, W. V., Mueller, H. J., Schilling, F., & Lauterjung, J. (2005). The influence of OH in coesite on the kinetics of the coesite-quartz phase transition. *American Mineralogist*, *90*, 36–43.

Liou, J. G., Zhang, R. Y., Ernst, W. G., Rumble, D., and Maruyama, S. (1998). High-pressure minerals from deeply subducted metamorphic rocks. In Hemley, R. J. Eds., Ultrahigh Pressure Mineralogy: Physics and Chemistry of the Earth's Deep Interior, 37, 33–96. Reviews in Mineralogy and Geochemistry, Mineralogical Society of America, Chantilly, Virginia.

Liu, Q., Hermann, J., & Zhang, J. (2013). Polyphase inclusions in the Shuanghe UHP eclogites formed by subsolidus transformation and incipient melting during exhumation of deeply subducted crust, *Lithos*, *177*, 91–109.

Massonne, H. J. (2001). First find of coesite in the ultrahigh-pressure metamorphic area of the central Erzgebirge, Germany. *European Journal of Mineralogy*, *13*, 565–570.

Massonne, H. J., & Nasdala, L. (2003). Characterization of an early metamorphic stage through inclusions in zircon of a diamondiferous quartzofeldspathic rock from the Erzgebirge, Germany. *American Mineralogist*, *88*, 883–889.

Mosenfelder, J. L., & Bohlen, S. R. (1997). Kinetics of the coesite to quartz transformation. *Earth and Planetary Science Letters*, *153*, 133–147.

Mosenfelder, J. L., Schertl, H. P., Smyth, J. R., & Liou, J. G. (2005). Factors in the preservation of coesite: The importance of fluid infiltration. *American Mineralogist*, *90*, 779–789.

Nagasaki, A. (1997). Petrology and Geochemistry of Su-Lu ultra high-pressure metamorphic rocks, China. *MSc Thesis*, Nagoya University (20 pp.).

Okay, A. I., Xu, S. & Sengör, A. M. C. (1989). Coesite from the Dabie Shan eclogites, central China. *European Journal of Mineralogy*, *1*, 595-598.

Palmeri, R., Frezzotti, M. L., Godard, G., & Davies, R. J. (2009). Pressure-induced incipient amorphization of α-quartz and transition to coesite in an eclogite from Antarctica: a first record and some consequences. *Journal of Metamorphic Geology*, *27*, 685–705.

Renders, P. J. N., Gammons, C. H., & Barnes, H. L. (1995). Precipitation and dissolution rate constants for cristobalite from 150 to 300 ˚C. *Geochimica et Cosmochimica Acta*, *59*, 77–85.

Rimstidt, J. D., & Barnes, H. L. (1980). The kinetics of silica-water reactions. *Geochimica et Cosmochimica Acta*, *44*, 1683–1699.

Schmalholz, S. M., & Podladchikov, Y. (2014). Metamorphism under stress: The problem of relating minerals to depth. *Geology*, *42*, 733–734.

Schmalholz, S. M., Medvedev, S., Lechmann, S. M., & Podladchikov, Y. (2014). Relationship between tectonic overpressure, deviatoric stress, driving force, isostasy and gravitational potential energy. *Geophysical Journal International*, *197*, 680–696.

Sheng, Y. M., Zheng, Y. F., Li, S. N., & Hu, Z. (2013). Element mobility during continental collision: insights from polymineralic metamorphic vein within UHP eclogite in the Dabie orogen. *Journal of Metamorphic Geology*, *31*, 221–241.

Smith, D. C. (1984). Coesite in clinopyroxene in the Caledonides and its implications for geodynamics. *Nature*, *310*, 641–644.

Taguchi, T., Enami, M., & Kouketsu, Y. (2016). Prograde evolution of Sulu UHP metamorphic rock in Yangzhuang, Junan region, deduced by combined Raman and petrological studies. *Journal of Metamorphic Geology*, *34*, 683–696.

Wang, L., Kusky, T. M., Polat, A., Wang, S., Jiang, X., Zong, K., Wang, J., Deng, H. & Fu, J. (2014). Partial melting of deeply subducted eclogite from the Sulu orogen in China. *Nature communications*, *5*, doi:10.1038/ncomms6604.

Wang, S., Wang, L., Brown, M., & Feng, P. (2016). Multi-stage barite crystallization in partially melted UHP eclogite from the Sulu belt, China. *American Mineralogist*, *101*, 564–579.

Wang, X., Liou, J.G. & Mao, H.K. (1989). Coesite-bearing ecologite from the Dabie Mountains in central China. *Geology*, *17*, 1085–1088.

Whitney, D. L., & Evans, B. W. (2010). Abbreviations for names of rock-forming minerals. *American mineralogist*, *95*, 185–187.

Yang, J. -J., & Smith, D. C. (1989) Evidence for a former sanidine–coesite–eclogite at Lanshantou, Eastern China, and the recognition of the Chinese "Su-Lu Coesite-Eclogite Province", Third International Eclogite Conference, Blackwell, *Terra Abstracts*, *1*, pp. 26.

Yang, J. -J., Godard, G., & Smith, D. C. (1998). K-feldspar-bearing coesite pseudomorphs in an eclogite from Lanshantou (Eastern China). *European Journal of Mineralogy*, *10*, 969–986.

Yang, J. -J., Huang, M. X., Wu, Q. Y., & Zhang, H. R. (2014a). Coesite-bearing eclogite breccia: implication for coseismic ultrahigh-pressure metamorphism and the rate of the process. *Contributions to Mineralogy and Petrology*, *167*, 1–17.

Yang, J. -J., Fan, Z. F., Yu, C., & Yan, R. (2014b). Coseismic formation of eclogite facies cataclasite dykes at Yangkou in the Chinese Su-Lu UHP metamorphic belt. *Journal of Metamorphic Geology*, *32*, 937–960.

Yang, J. -J., Zhang, H. R., Chen, A. P., & Huang, M. X. (2017). Petrological evidence for shock-induced high-P metamorphism in a gabbro. *Journal of Metamorphic Geology*, *35*, 121–140.

Ye, K., Yao, Y., Katayama, I., Cong, B., Wang, Q., & Maruyama, S. (2000). Large areal extent of ultrahigh-pressure metamorphism in the Sulu ultrahigh-pressure terrane of East China: new implications from coesite and omphacite inclusions in zircon of granitic gneiss. *Lithos*, *52*, 157–164.

Zhang, R. Y., Liou, J. G., Iizuka, Y., & Yang, J. S. (2009). First record of K-cymrite in North Qaidam UHP eclogite, Western China. *American Mineralogist*, *94*, 222–228.

FIGURE AND TABLE CAPTIONS

FIGURE 1. Geological map of the Su-Lu UHP metamorphic terrane. YQW, Yantai–Qingdao–Wulian Fault; JXF, Jiashan–Xiangshui Fault.

FIGURE 2. (a) Manganese (Mn), calcium (Ca), magnesium (Mg), and iron (Fe) X-ray maps of complex zoning in garnet. **(b)** Compositional profiles of complex-zoned garnet. **(c)** Ca X-ray map of complex zoned garnet containing kyanite with coesite. **(d)** Relict coesite inclusion in a kyanite grain from the outer segment of garnet under plane-polarized light. **(e)** Backscattered electron (BSE) images of the Yangzhuang UHP eclogite showing a pseudomorph after coesite with radial cracks in the surrounding host garnet.

FIGURE 3. Microphotograph images of the pseudomorph with radial cracks in the outer segment of the garnet host under **(a)** plane-polarized light and **(b)** cross-polarized light. **(c)** BSE image of pseudomorphs with radial cracks in the surrounding host garnet. X-ray maps of the pseudomorph in garnet for **(d)** silicon (Si), **(e)** potassium (K), and **(f)** magnesium (Mg). **(g)** BSE image of an anhedral SiO_2 phase coexisting with fibrous phases in the pseudomorph. The red-dashed box shows the predefined partial area of FIB.

FIGURE 4. Raman spectra measured at SiO_2 (Spot 1 and 2) and fibrous (Spot 3) phases in the pseudomorph after coesite. Raman spectrum of the coesite inclusion (Spot 4) within a kyanite grain from the outer segment of the garnet. Raman spectra of the SiO_2 glass (from Ivanda et al. 2003) and standard quartz are also presented.

FIGURE 5. TEM results of a portion of the pseudomorph consisting of APSI and KFSS phases: **(a)** the BF-TEM image of a cross-section of the pseudomorph after coesite, **(b)** the HAADF-STEM image of textures of the pseudomorph, **(c)** chemical compositions of the worm-like APSI and KFSS phases using TEM-EDS, **(d)**, **(e)** the BF-TEM images and SAED pattern of the worm-like APSI phases, **(f)** the BF-TEM image and the SAED pattern of nanocrystalline quartz in the APSI phase, **(g)** the BF-TEM image and the SAED pattern of submicrocrystalline quartz, and **(h)** the BF-TEM image and the SAED pattern with weak ring

patterns of the KFSS phase. The SAED patterns of the areas indicated by white circles are shown as insets in Figure 5d–h.

FIGURE 6. (a) Pressure-temperature (P-T) diagram showing the schematic retrograde P-T path (from Wang et al. 2014) followed by coesite inclusions within garnet and Su-Lu UHP rocks. Coesite inclusions undergo rupture and decompression (limit of coesite preservation in the quartz stability field from Mosenfelder and Bohlen 1997). Transition curve of Qz = Coe was calculated using THERMOCALC ver. 3.33 (Holland and Powell 1998, updated June 2009). **(b)** Enlarged view of the diagram of the retrograde P-T path of Su-Lu UHP rocks and schematic illustration of the probable precipitation style from the metamorphic fluid during the exhumation. The APSI and KFSS phases within the pseudomorph were formed by reactions involving a supercritical fluid during the following processes: (stage 1) the development of radial cracks within the host garnet by the phase transition of coesite to quartz -> (stage 2) the decomposition of a part of the pseudomorph by the infiltration of supercritical fluid -> (stage 3) the precipitation of the KFSS phases from the SiO_2-rich fluid probably promoted by the state change of the metamorphic fluid from supercritical and/or subcritical to normal -> (stage 4) rapid precipitation of the APSI phase under a metastable (non-equilibrium) state, such as a quenching reaction, during a later stage of exhumation. The APSI and KFSS phases correspond to the dark-colored areas under plane-polarized light (Figure 3a).

TABLE 1. Bulk-rock chemical composition of the eclogite sample 95ZYa.
N97, Nagasaki (1997)

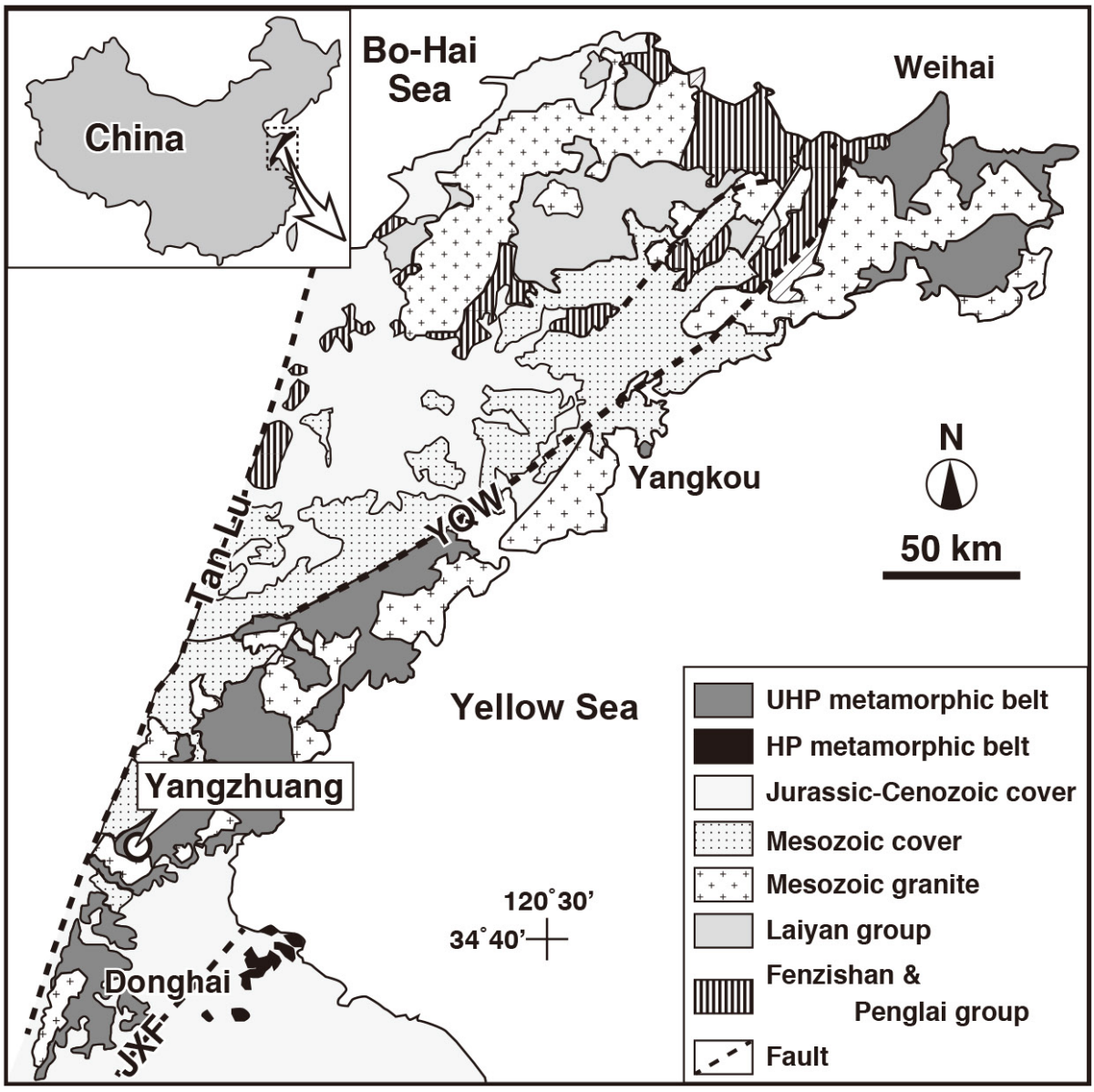

Figure 1
Taguchi et al.

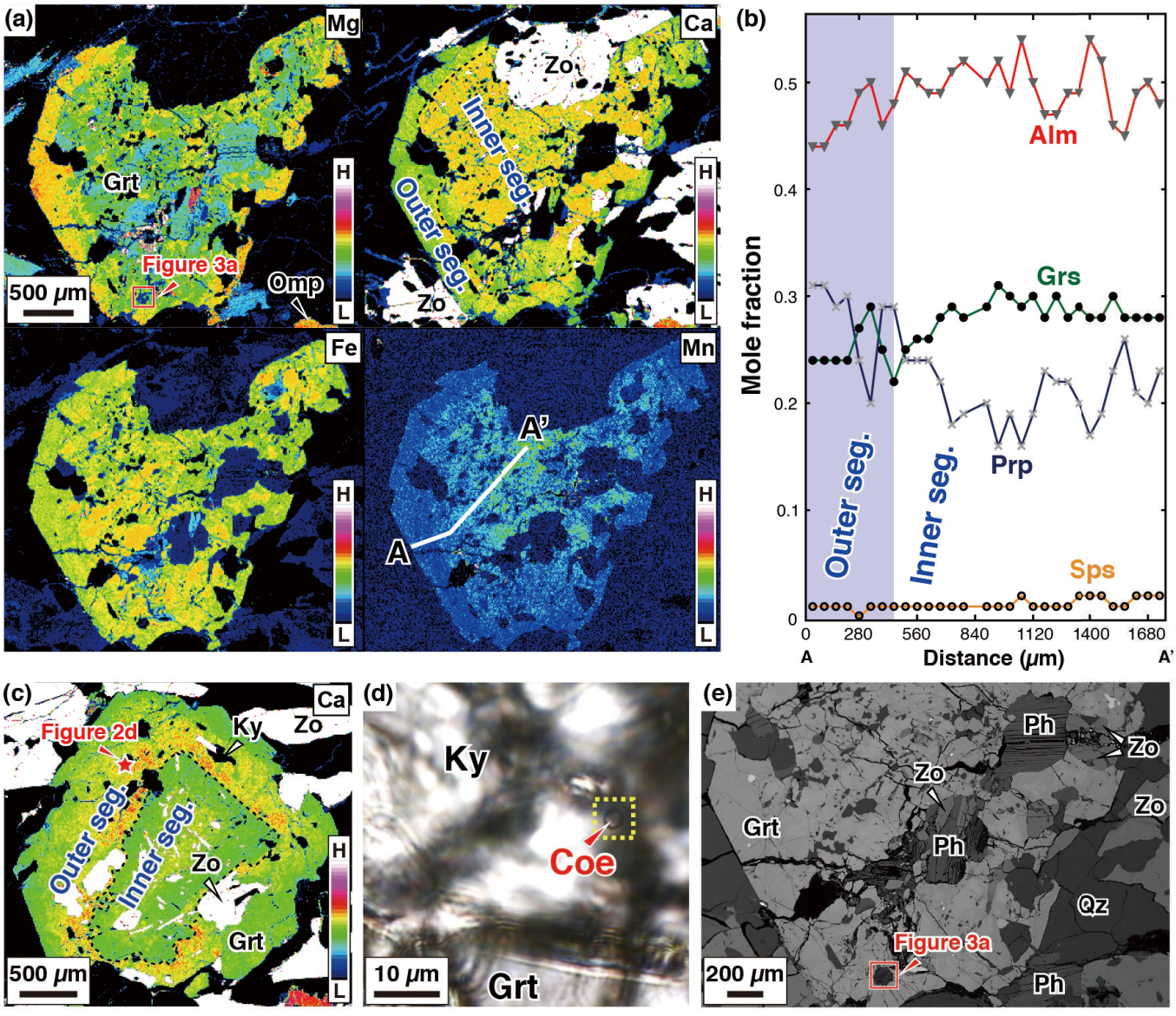

Figure 2
Taguchi et al.

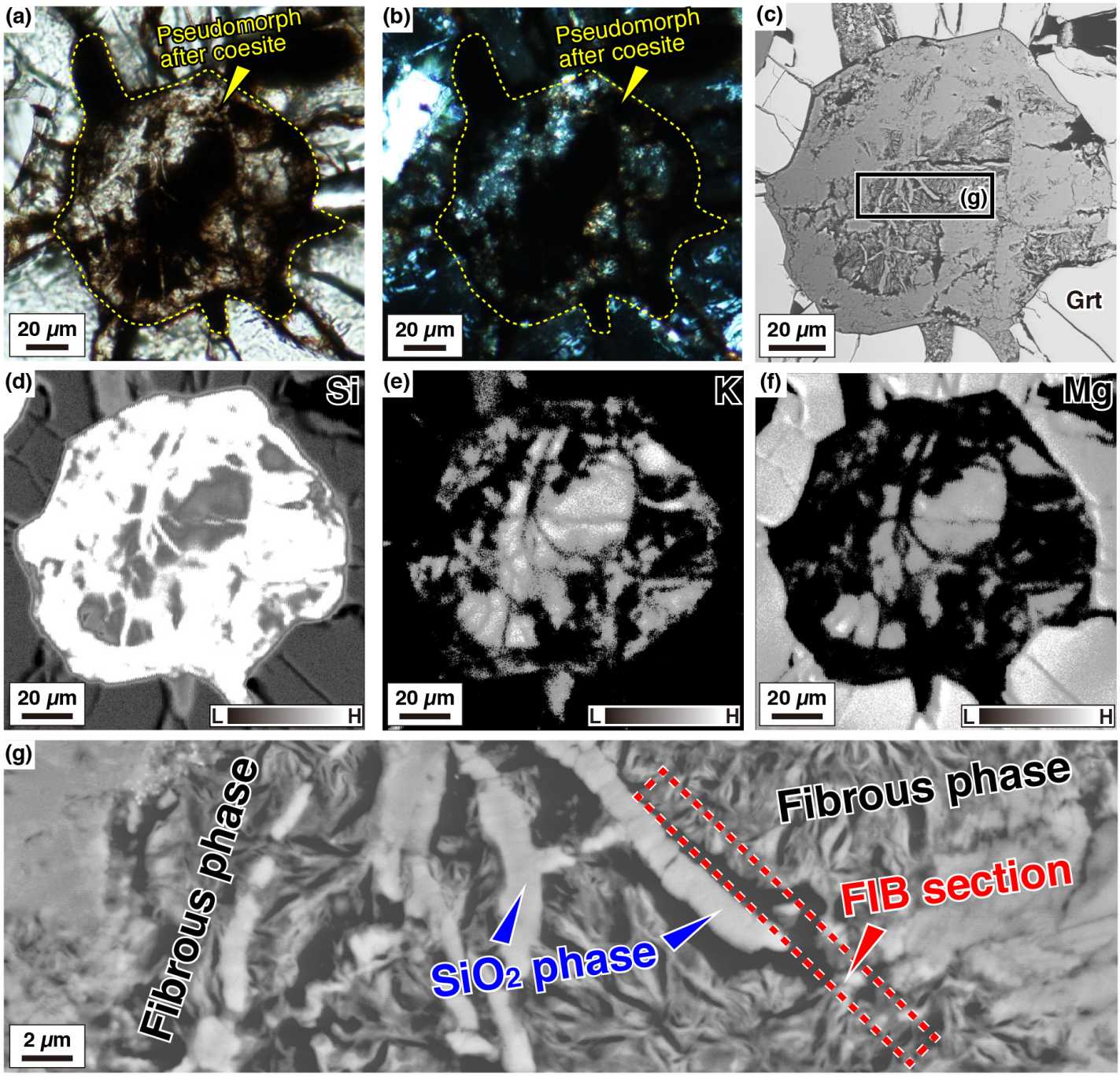

Figure 3
Taguchi et al.

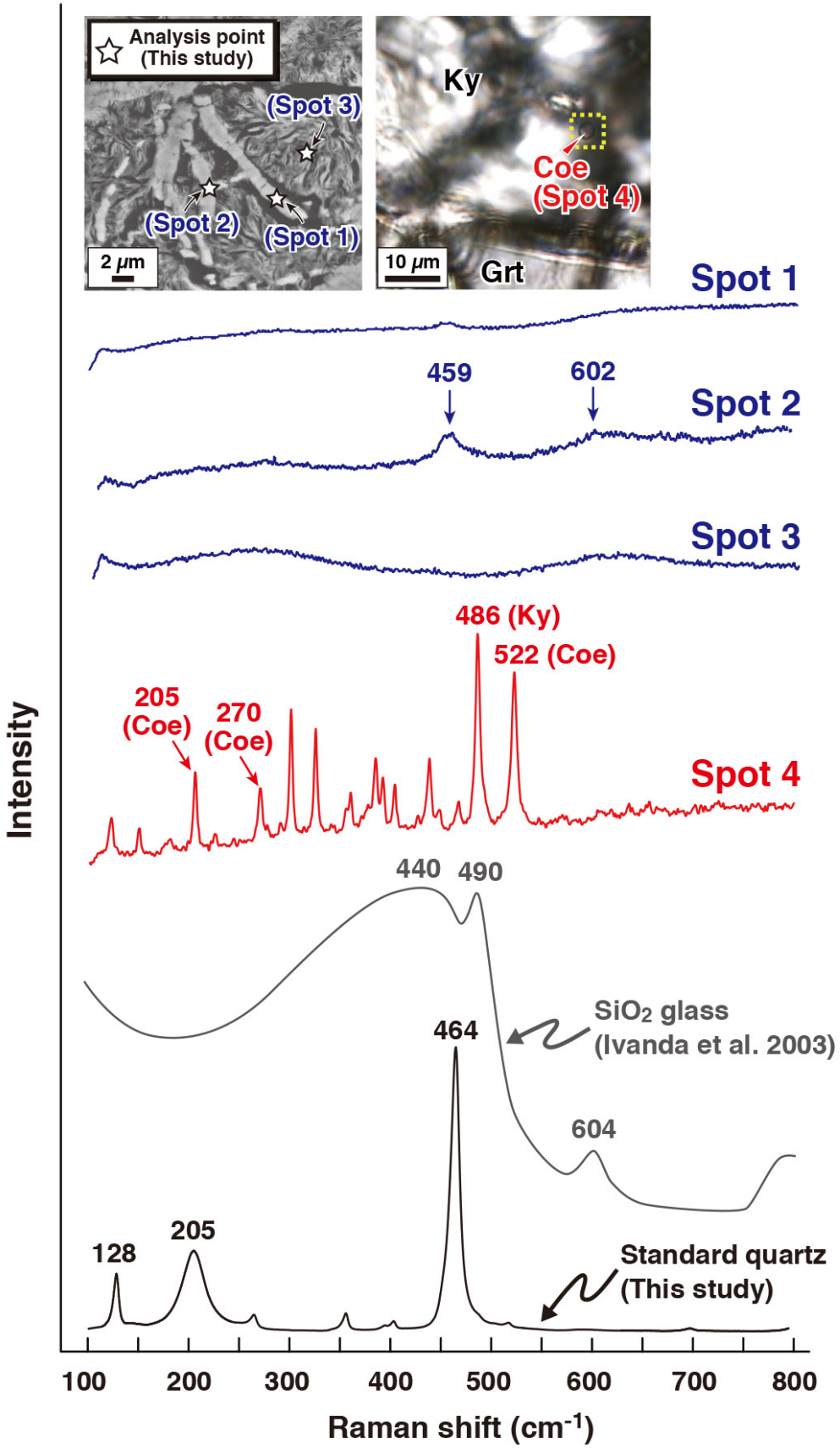

Figure 4
Taguchi et al.

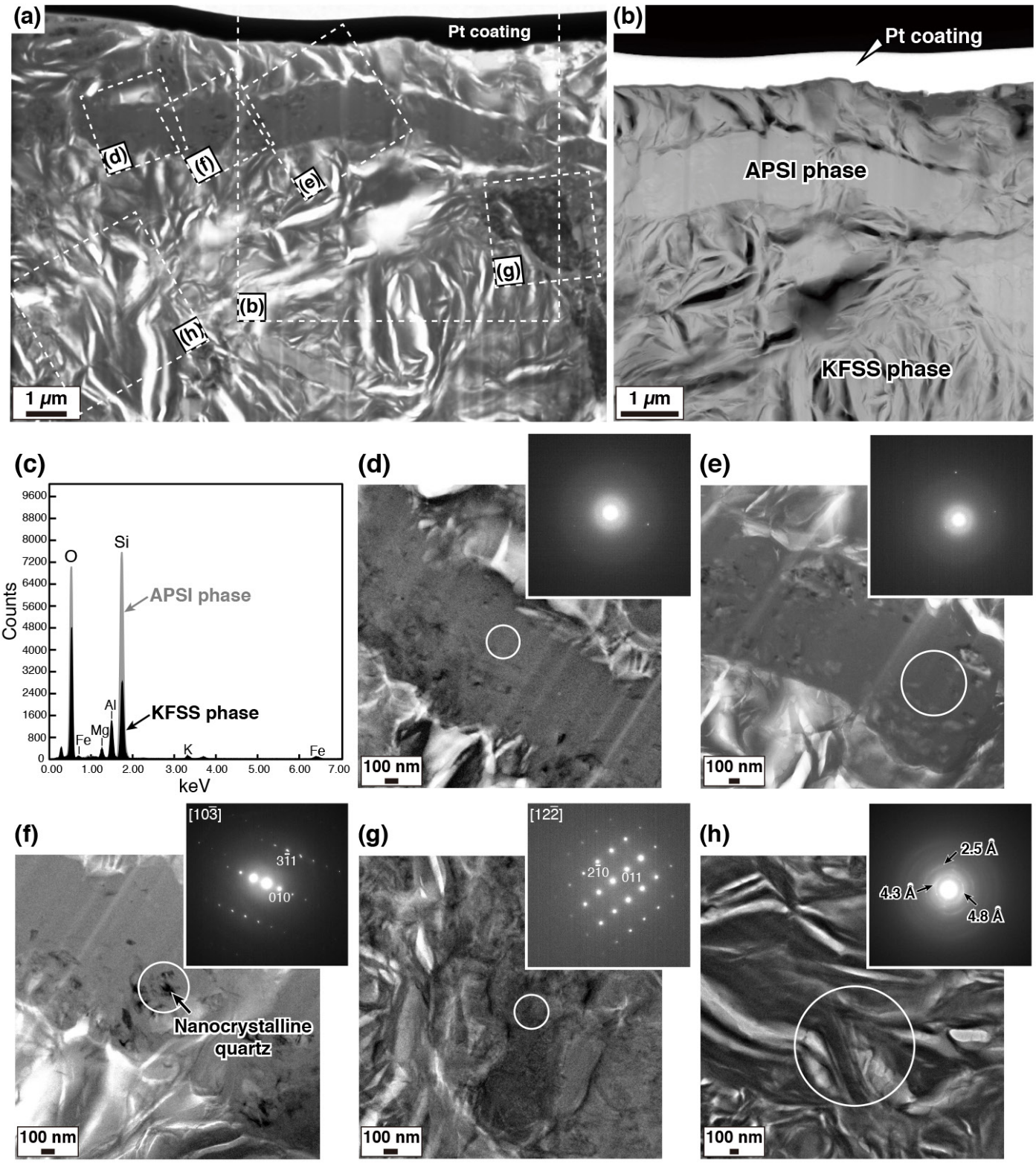

Figure 5
Taguchi et al.

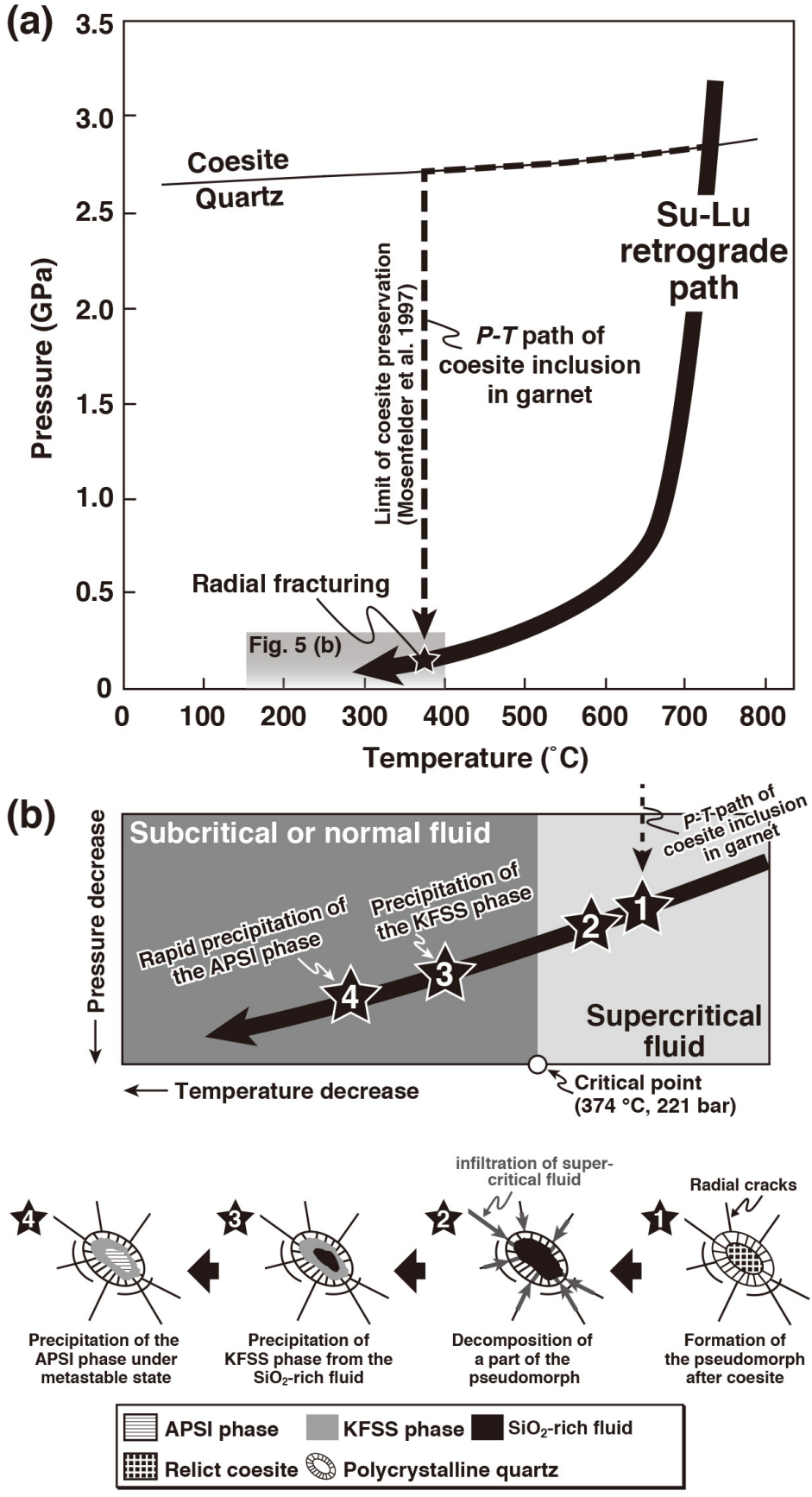

Figure 6
Taguchi et al.

Table 1. Bulk-rock chemical composition of the eclogite sample 95ZYa.

Locality	Yangzhuang
Sample	95ZYa N97
SiO_2 wt.%	49.50
TiO_2	0.78
Al_2O_3	27.20
Fe_2O_3	4.13
MnO	0.05
MgO	2.01
CaO	12.60
Na_2O	0.72
K_2O	1.10
P_2O_5	0.19
Total	98.28
Cr ppm	87
Co	19
Ni	39
Cu	28
Zn	23
Ga	25
Rb	21
Sr	1688
Y	20
Zr	122
Nb	5
Ba	437
Pb	6
Th	4

N97, Nagasaki (1997)